Impurity modes in the optical stop bands of doped colloidal crystals

Ranjit D. Pradhan, İ. İnanç Tarhan, and George H. Watson
Department of Physics and Astronomy, University of Delaware, Newark, Delaware 19716
(Received 12 June 1996)

Colloidal suspensions of charged polystyrene microspheres can self-organize into colloidal crystals, providing a three-dimensional periodic dielectric medium suitable for the study of photonic band structure effects in the infrared, near-infrared, and visible wavelength regimes. Light propagation along any particular direction in such a system displays bands of frequencies for which the propagation of light is strongly inhibited. Substitutional doping of these colloidal crystals with scatterers of slightly different size or different dielectric strength introduces optical disorder into these crystals which is manifested by the appearance of impurity modes within the optical stop bands. These defect modes can be tuned by appropriate selection of the defect volume and the dielectric constants of the dopants. Widening of optical stop bands with increasing impurity peak heights was observed in the doped crystals. [S0163-1829(96)02644-6]

Electromagnetic wave propagation in an extended periodic dielectric medium, a so-called photonic crystal, can be strongly inhibited for a certain frequency range, along any direction exhibiting dielectric periodicity. A structure with a periodic arrangement of high and low dielectric regions which forbids light propagation in all directions, in a finite band of frequencies, for all polarizations, is called a photonic band gap (PBG) crystal. Since the idea of a three-dimensional (3D) PBG crystal was proposed,[1,2] vigorous activity in the field has uncovered many structures which display a full PBG.[3,4] PBG materials promise numerous potential applications,[5] some of which have already been harnessed in the form of high efficiency microwave antennas.[6] Many of the projected optical regime applications involve the suppression of spontaneous emission which will lead to more efficient solid-state devices.[5] Recently, 3D metallic[7] and metallodielectric[8] PBG materials, with microwave and millimeter wave applications in mind, have been fabricated.

The application of photonic crystals will be enhanced by ''doping'' them with impurities to generate defect states.[9–11] The addition or removal of high dielectric material from an existing PBG structure is analogous to the addition of donor or acceptor impurities in the semiconductor case. If incorporated into semiconductor lasers, PBG materials can suppress spontaneous emission, leading to a thresholdless laser, while a defect mode could be created to allow passage of the stimulated emission. A high-Q single-mode cavity could be created by the introduction of a local defect in a PBG structure.[9]

The scale invariance of Maxwell's equations indicates that in order to obtain a complete PBG in the optical regime, one needs to scale down prospective structures until a dielectric periodicity over distances comparable to optical wavelengths is achieved. 3D PBG crystals with lattice parameters approaching hundreds of micrometers have been fabricated; ways of miniaturizing these crystals further have been suggested, and there is a growing recognition that the optical regime may best be approached by employing self-ordering materials.[4]

Self-organizing colloidal crystal systems provide a means of achieving periodic dielectric structures with feature sizes comparable to optical wavelengths.[12] For example, colloidal suspensions of polystyrene (PS) microspheres in water can be made to crystallize in either fcc or bcc lattices by controlling the volume fraction of solids in suspension. This system does not possess a full PBG owing to the relatively low dielectric contrast between polystyrene and water ($\epsilon_{\text{contrast}}=1.44$). However, optical stop bands with several orders of magnitude attenuation in the transmission coefficient have been observed, and the photonic band structure of PS fcc colloidal crystals has been extensively studied.[13,14] These self-assembling structures do not necessitate the use of elaborate microfabrication techniques, making them interesting candidates for study of light propagation in 3D periodic dielectric media at infrared, near-infrared, and visible wavelengths. Doping the colloidal crystals, with either PS microspheres of smaller or larger diameter than those in the host or microspheres of a material with different dielectric constant, introduces optical disorder in the system, leading to the appearance of impurity states.

The colloidal crystals under investigation were prepared by diluting suspensions of charged PS microspheres to the volume fraction calculated to yield the desired lattice parameter. The typical microsphere diameters were between 0.100 and 0.250 μm, with a typical standard deviation of 4% in the diameter.[15] The required amount impurity microsphere suspension was added to the starting solution in the case of doped samples. The maximum impurity microsphere number fraction (fraction of the total number of microspheres) was 10%. The PS microspheres have negatively charged end groups and positively charged counterions forming an electrical double layer. Stray ions, which effectively screen the charged microspheres, are also present in the solution. Tumbling the solution with mixed bed ion exchange resin leads to a reduction in stray ion concentration. This promotes intermicrosphere interaction, precipitating a phase transition into an ordered state. The crystal structure is fcc for the range of microsphere volume fractions used. At the onset of crystallization, the milky white colloidal suspension turns irridescent owing to Bragg diffraction of light off the various crys-

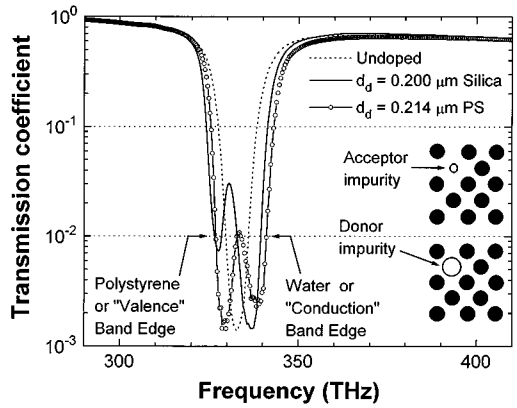

FIG. 1. Near-infrared transmission spectra. The dotted curve is a transmission spectrum for an undoped polystyrene (PS) colloidal crystal of lattice parameter $a=0.580$ μm and host microsphere diameter $d=0.173$ μm. The plain solid curve and the solid curve with open circles show the spectra for crystals doped with 0.200-μm silica (2% number fraction) and 0.214-μm polystyrene (10% number fraction), respectively. The polystyrene and the water band edges are also shown. The insets elucidate the notion of an acceptor and a donor impurity for this system if PS microspheres of different diameters are used as dopants.

tal planes formed near the walls of the sample vials. At this stage, the exact volume fraction of this solution was determined by weighing a portion of the dried suspension. The solution was injected into specially fabricated cells which have a thin working region ($\sim$0.5 mm) surrounded by a reservoir for the colloidal suspension. The fcc (111) planes preferentially orient parallel to the glass windows of the crystal cell, which facilitates the crystal alignment for transmission measurements. Formation of mm-size single crystals is promoted by shear annealing,[12,16] which involves rocking these crystals about an axis perpendicular to the (111) planes, with a peak-to-peak amplitude of 60° at a frequency of about 45 Hz. The quality and orientation of the crystals was confirmed by using the Kossel line patterns from the crystals as guides.[13] The transmission spectra along the [111] direction were obtained using a modified UV/visible/near IR spectrophotometer with a collimated beam and standard lock-in detection techniques.

Figure 1 shows the experimental transmission spectra, along the [111] direction, for both undoped and doped colloidal crystals. The transmission spectrum of an undoped crystal of 0.173-μm PS host ''atoms'' is compared with that for crystals doped with 0.200-μm diameter silica microspheres and 0.214-μm diameter PS microspheres, respectively. In all crystals studied, over two orders of magnitude attenuation in the transmission coefficient is observed in the optical stop band.[17] Doping this crystal introduces optical disorder into the otherwise periodic dielectric medium, resulting in the appearance of impurity peaks within the optical stop bands, as seen in Fig. 1. The insets indicate the definition of ''acceptor'' and ''donor'' impurities in this system. Replacement of a host PS microsphere by one of lower optical volume (either smaller diameter PS or a microsphere of lower refractive index than PS such as silica) constitutes an acceptor impurity. Similarly, a donor impurity can be introduced by substitution with a microsphere of higher optical volume.

The position of the impurity peak in Fig. 1 is different for the two different impurity ''strengths.'' The donor impurity (0.214-μm PS) peak is relatively closer to the high-energy edge (''water'' or ''conduction'' band edge) of the optical stop band, while the acceptor impurity (0.200-μm silica) peaks is closer to the low-energy edge (''polystyrene'' or ''valence-band'' edge). The impurity strength can be changed either by changing the relative impurity size or by changing the impurity refractive index. Colloidal crystals offer some flexibility in achieving variation of impurity sizes, either by changing the impurity microsphere diameter, keeping the lattice parameter and the host microsphere diameter fixed, or by keeping the diameter of the impurity fixed and scaling down the lattice parameter of the host. However, to compare the transmission through crystals with different lattice parameters, it is necessary to normalize the frequencies to units of the speed of light divided by the lattice parameter (c/a).

Two factors complicate the determination of the lattice parameter a for the doped crystals. First, the crystal formed in the thin working region of the cell, undergoes an apparent contraction in the lattice parameter by a factor of 0.92 ± 0.02 from that expected from purely volume fraction determination. This was determined by comparing the lattice parameter obtained spectroscopically from the transmission curves for an undoped crystal with the one obtained from the measured volume fraction. From the transmission spectra obtained at various points on the crystal, we believe that the actual lattice parameter fluctuates by 3% across the crystal ($\sim$10 mm). Therefore the lattice parameter at the scanning site needs to be extracted spectroscopically. Second, as seen in Fig. 1, there is a conspicuous widening of the doped optical stop band which may not be symmetric. The method of extraction of the lattice parameter a from the transmission spectrum addresses this issue, and is outlined below.

The lattice parameter is related to the transmission minimum wavelength λ_o by Bragg's law

$$2d_{111}n_c=\lambda_o, \tag{1}$$

where d_{111} is the separation between the (111) planes, and n_c is the average crystal refractive index. In PBG crystals with large dielectric contrast, Bragg's law is an approximation.[18] However for the relatively low dielectric contrast in the polystyrene colloidal crystals, Bragg's law is a good approximation. The average crystal dielectric constant ϵ_c can be approximated by

$$\epsilon_c=f\epsilon_p+(1-f)\epsilon_w, \tag{2}$$

where ϵ_p and ϵ_w are the dielectric constants of polystyrene and water, and f is the volume fraction of the polystyrene microspheres in the crystal. For the fcc lattice, the volume fraction f is related to the lattice parameter a $(a=d_{111}\sqrt{3})$ through the following relations:

$$f=\frac{2\pi}{3}\frac{d^3}{a^3}, \tag{3}$$

d being the diameter of the polystyrene microspheres. The following equation can be solved to obtain the average crystal refractive index $n_c=\sqrt{\epsilon_c}$ at the transmission minimum wavelength λ_o (frequency $\nu_o=c/\lambda_o$),

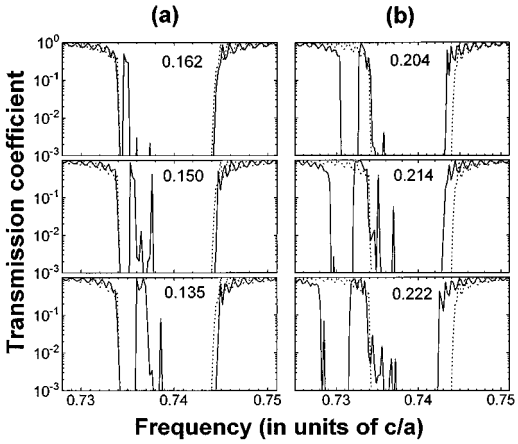

FIG. 2. TMM calculation of [100] transmission spectra for crystals doped with impurity microspheres of diameter different than the host, with lattice parameter $a=0.582$ μm and microsphere diameter $d=0.173$ μm. One impurity microsphere per unit cell is introduced substitutionally (25% impurity number fraction). (a) Case with acceptor impurities with diameters $d_d=0.162$, 0.150, and 0.135 μm. (b) Case of donor impurities with diameters $d_d=0.204$, 0.214, and 0.222 μm. The dotted curve shows the undoped case, while the solid curves are for doped crystals. The frequency is expressed in units of the speed of light divided by the lattice parameter (c/a).

$$n_c{}^3+a_1 n_c{}^2+a_3=0. \tag{4}$$

The constants a_1 and a_3 in Eq. (4) depend on the wavelength λ_o, the host microsphere diameter d, and the refractive indices n_p and n_w according to the following relations:

$$a_1=-\frac{\lambda_o{}^3}{\zeta},\quad a_3=\frac{\lambda_o{}^3 n_w{}^2}{\zeta},\quad \zeta=\frac{16\pi}{9\sqrt{3}}d^3(n_p{}^2-n_w{}^2).$$

The dispersion in the refractive indices of polystyrene and water was also taken into account. Thus if λ_o can be determined from the transmission spectra, one can determine n_c and thus the lattice parameter a.

While λ_o can be directly read from the transmission spectrum for the undoped samples, its determination for the doped samples is not straightforward on account of the band widening seen in Fig. 1. Transfer-matrix-method (TMM) (Ref. 19) calculations of the fcc [100] transmission coefficient were used to guide our lattice parameter determination. The [100] transmission coefficient was calculated using the source code provided by Pendry and MacKinnon with some minor modifications. The transmission spectra, through a total of 512 unit cells, were simulated for both the undoped and substitutionally doped crystals. The diameter of the substitutional impurity microsphere was varied for both the donor and the acceptor cases. Dispersion in the refractive index of both polystyrene[20] and water was accounted for in these calculations.

Introduction of the impurities considerably alters the structure of the transmission spectrum with impurity modes appearing within the optical stop band. Figure 2(a) shows the results of these calculations for the acceptor case. As the impurity microsphere diameter is increased from 0.135 to 0.162 μm, it approaches the diameter of the host ''atoms'' and constitutes a reduction in the optical disorder. The impurity mode in the band gap moves toward the polystyrene band edge, and the overall width of the impurity peaks shrinks. There is some band widening as a result of impurities. The calculations for the donor impurity case are shown in Figure 2(b). As the diameter of the donor impurity microsphere increases from 0.204 to 0.222 μm, the optical disorder increases, the impurity peak moves away from the water band edge, and the impurity peak broadens. Unlike the acceptor case where the band widening is small, there is considerable band widening in this case, with the water band edge remaining relatively stationary, while the polystyrene band edge moves outward toward the low-energy side. This was used as a guide for the analysis of experimental data discussed later in this paper. For a relatively low dielectric contrast system, this overall behavior of the impurity peak movement and the band widening with changing impurity ''strength'' is expected to remain the same in all directions with minor differences. Therefore, it is reasonable to expect similar behavior of impurity peaks along the [111] direction.

For the doped crystals, the water band edge is expected to be relatively immune to the effects of band widening in the presence of impurities. Therefore, it seems reasonable to determine the lattice parameter a using the observed water band edge frequency $\nu_+=c/\lambda_+$. For this purpose an analytical model[21,22] was used, where the center frequency predicted for the undoped samples is in good agreement with Bragg's law. The model predicts the water band edge frequency ν_+ and the polystyrene band edge frequency ν_- for the [111] optical stop band to be

$$\omega_\pm=2\pi\nu_\pm=\frac{1}{2}\frac{cG}{\epsilon_c\pm U_G}, \tag{5}$$

where

$$G=2\pi\sqrt{3}/a,\quad U_G=\frac{2}{3\sqrt{3}\pi^2}(\epsilon_p-\epsilon_w)(\sin\xi-\xi\cos\xi),$$

$$\xi^3=3(\sqrt{3})^3\pi^2 f/2.$$

The center frequency $\nu_o=\frac{1}{2}(\nu_++\nu_-)$ corresponding to the observed water band edge frequency ν_+ was determined using these expressions. By solving Eq. (4) the crystal refractive index and consequently the lattice parameter was determined for each individual transmission spectrum, and the frequencies were converted to units of c/a.

Figure 3 shows the transmission spectra for the acceptor impurities, with frequencies normalized as outlined above. Note that the difference in impurity strength for the spectra shown comes by virtue of difference in the impurity refractive index, impurity microsphere diameter, and the sizes of the impurity relative to the lattice parameter. All three factors were utilized to realize the variation in acceptor impurity ''strengths.'' Figure 4 shows the result of changing the PS donor microsphere diameters. Increasing the donor impurity diameter leads to the impurity peak moving away from the water band edge.

The TMM calculations show systematic changes in impurity peak widths with changing impurity microsphere diameters. In the experimental transmission curves of Figs. 3 and 4 this is not evident. It is possible that the $\sim$4% deviation in

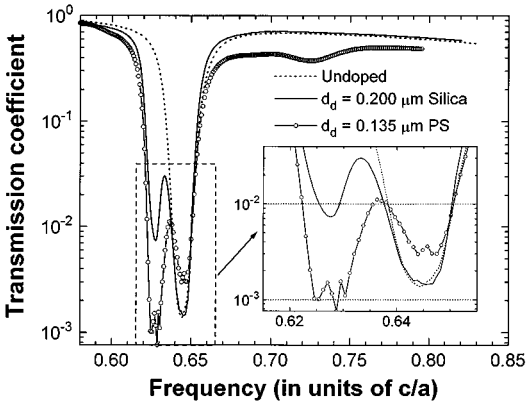

FIG. 3. Near-infrared transmission spectra for crystals with acceptor impurities. All curves have been normalized, so that the frequency is expressed in units of the speed of light divided by the lattice parameter (c/a). The undoped crystal (dotted curve) has a lattice parameter of $a=0.581$ μm with a host microsphere diameter $d=0.173$ μm. The solid curve is for a crystal doped with 0.200-μm silica (2% number fraction) in a 0.173-μm host, while the solid curve with circles shows the case of 0.135-μm polystyrene impurity microspheres (10% number fraction) in a 0.162-μm host. The inset shows the impurity region magnified.

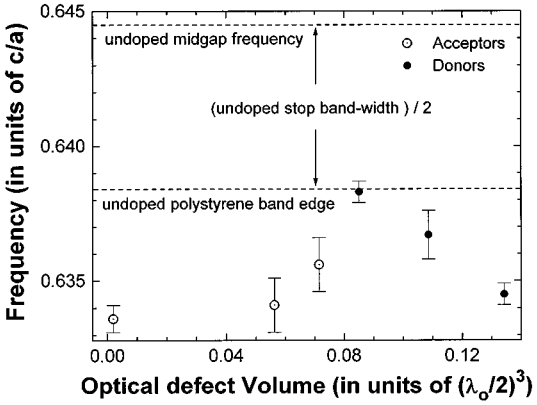

FIG. 5. Tuning the impurity mode. This figure shows the variation of the impurity mode frequency with the optical defect volume. The solid circles are for the donors, while the open circles are for the acceptor impurities. The figure shows the overall behavior of the impurity peaks with changing impurity ''strengths.'' The midgap, and the polystyrene band-edge frequencies for undoped crystals, have been marked to indicate the overall variation of the peak positions compared to the undoped bandwidth. There is some uncertainty regarding the exact positions of the defect peaks relative to the undoped optical stop band. The error bars represent deviations observed between scans on the same or different crystals.

both the host and the impurity microsphere diameter smears this effect. It is tempting to draw more inferences about this system from the TMM calculations. However, it is necessary to bear in mind that the TMM calculations simulate the transmission spectra for one impurity microsphere in every unit cell (25% concentration). Further, the impurities in our simulated structure are periodic. Since roughly one in every ten lattice sites is occupied by impurities in the case of the prepared samples, it is unlikely that the impurities themselves form an ordered array. The TMM calculations also do not adequately model the deviations in the host microsphere diameters.

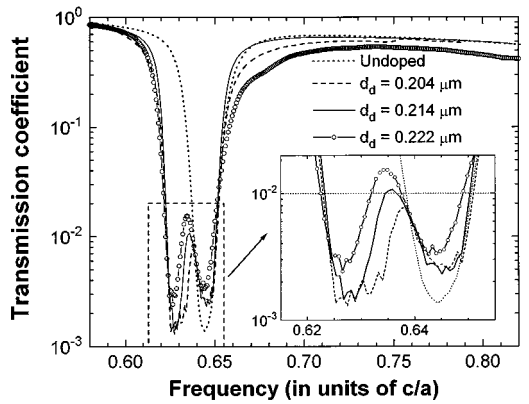

FIG. 4. Near-infrared transmission spectra for crystals with polystyrene donor impurities. All curves have been normalized so that the frequency is expressed in units of the speed of light divided by the lattice parameter (c/a). The undoped crystal has a lattice parameter of $a=0.581$ μm. The host microsphere diameter $d=0.173$ μm. The dotted curve shows the undoped crystal transmission spectrum, while the others show the same for dopant microspheres of diameters $d_d=0.204$, 0.214, and 0.222 μm (10% number fraction). The inset shows the impurity region magnified.

An interesting question arises as to the nature of the silica impurity. Does the silica impurity constitute a donor or an acceptor? The diameter of the silica microspheres (0.200 μm) is larger than the host PS microspheres (0.173 μm), while the refractive index of the silica microspheres (1.37) (Ref. 23) is lower than that of polystyrene. To resolve the question of whether this constitutes a donor or an acceptor impurity, one needs to compare the 0.200-μm silica-doped crystals (Fig. 3), with those doped with 0.204-μm PS microspheres (Fig. 4). Both these have the same 0.173-μm host microspheres. If the silica microsphere constituted a donor impurity, the corresponding impurity mode is expected to appear closer to the water band edge than the 0.204-μm PS-doped crystal. Since the silica impurity peak in the optical stop band appears near the polystyrene band edge, one can conclude that it behaves like an acceptor instead of a donor.

Since the impurity can have a refractive index different from either the high- (polystyrene) or low-index (water) regions of the periodic dielectric structure, it is appropriate to consider the optical volume of the impurity instead of its actual volume. The impurity volume is thus defined as

$$V_d=\frac{\pi}{6}|(n_d d_d)^3-(n_p d)^3|, \tag{6}$$

where n_d and n_p are the refractive indices, and d_d and d are the diameters of the impurity and the host microspheres, respectively. Figure 5 shows the variation in the position of the defect states, relative to the undoped water band edge, as a function of the optical defect volume V_d normalized to

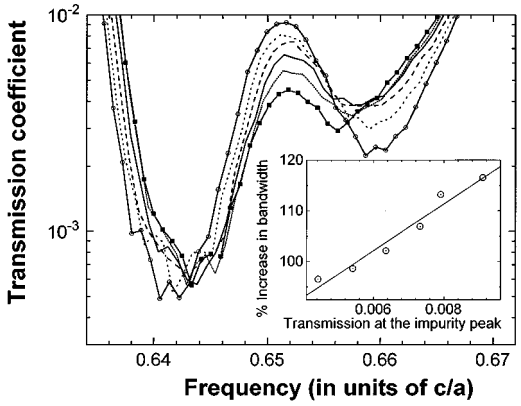

FIG. 6. Increasing stop band widening with increasing impurity peak height. The various curves show the transmission spectra at various points on a crystal with lattice parameter $a=480$ μm, host microsphere diameter $d=0.162$ μm, and impurity microsphere of diameter $d_d=0.135$ μm. The inset shows the variation of the [111] optical stop bandwidth (expressed as a percentage of the undoped stop bandwidth) with height of the impurity peak. Note that the position of the impurity peak remains fixed for the various curves shown.

$(\lambda_o/2)^3$. The total variation in the position of the donor impurity peaks is a significant fraction of the undoped band gap. Clearly, the defect state frequency can be ''tuned'' by appropriately selecting the volume and the dielectric constants of the impurity microspheres. It appears that the impurities widen the stop band by shifting the polystyrene band edge toward lower frequencies, and that most of the interesting impurity effects occur in this widened part of the optical stop band.

Since the colloidal crystal solution was thoroughly mixed before injecting it into the sample cells, there is no reason to expect a nonuniform distribution of impurities in the crystal. The impurity features in the optical stop band were typically observed to be uniform across the entire single crystal; such samples served our previously discussed measurements. However, some crystals displayed nonuniform impurity peak heights, as shown in Fig. 6. In such cases, there appears to be a correlation between the impurity peak height and the overall widening of the optical stop band. The inset of Fig. 6 shows the variation of band widening with increasing impurity peak height. Band widening has been known to occur in the presence of high impurity concentrations in the semiconductor case, and has also been observed in calculations of two-dimensional photonic band structure of dielectric cylinders in air.[24] Note that the position of the impurity peak stays the same in all the spectra shown in Fig. 6. This suggests that, for studying the effect of changing impurity microsphere diameter, maintaining exactly the same impurity concentration may not be critical. Very high impurity concentrations are likely to cause large changes in the local lattice parameter, thereby modifying the overall optical stop band structure. In semiconductors, it has been known that the introduction of large impurity atoms leads to a strain in the lattice which modifies the energy gap.[25]

In conclusion, we presented a systematic study of impurity modes in the optical stop bands of polystyrene colloidal crystals. Since this system is not close packed, it offers considerable flexibility in the choice of lattice parameters and volume fractions. In addition, the impurity strength can be varied by appropriate selection of the diameter and/or the refractive index of the impurity microspheres. An acceptor impurity mode tends to shift toward the water band edge with increasing impurity strength. The donor impurity mode shifts away from the water band edge. This behavior of the impurity modes is consistent with the overall trends seen in our TMM calculations. The silica impurity microsphere, with a larger diameter than the host ''atoms'' but having a lower refractive index, does not have a semiconductor analog. From the position of the silica impurity peak in the optical stop band, it can be concluded that a microsphere larger than the host microspheres constitutes an acceptor impurity provided its index of refraction is smaller than that of polystyrene, even though its optical volume is larger than the host microsphere.

The presence of impurities leads to a significant widening of the optical stop band, which is proportional to the impurity peak height. In most of the work reported on impurity modes in photonic crystals, the number of unit cells used for such a study has been small. In the colloidal crystal system, although the dielectric contrast is low, the presence of $\sim 10^3$ (111) planes along the direction of incidence permits the study of crystals with larger numbers of sampled impurities. This mimics the widening of band gaps and the formation of bands of impurities similar to the case of semiconductors with high impurity concentrations.

An exciting possibility is the study of nonlinear optical effects in these systems. This can be realized by the introduction of optical nonlinearity into these doped crystals using a background liquid (instead of water) and/or particles with intensity-dependent dielectric constants. When doped, these nonlinear systems can have tunable defect states in the optical stop bands, the frequency of which can be controlled by changing the intensity of the pump laser.

We would like to thank Professor J. B. Pendry at the Imperial College, London, and his collaborators for making the TMM source code ''opal'' available to us, and Dr. Andrew Ward for his on-line help. This work was supported by the National Science Foundation under Grant No. DMR-9510460.

[1] E. Yablonovitch, Phys. Rev. Lett. **58**, 2059 (1987).
[2] S. John, Phys. Rev. Lett. **58**, 2486 (1987).
[3] Special review issues: C. M. Bowden, J. P. Dowling, and H. O. Everitt, J. Opt. Soc. Am. B **10** (1993); G. Kurizki and J. W. Haus, J. Mod. Opt. **41** (1994).
[4] For a recent review, *Photonic Band Gap Materials*, edited by C. M. Soukoulis (Kluwer Academic, Dordrecht, 1996).
[5] E. Yablonovitch, J. Mod. Opt. **41**, 173 (1994).
[6] E. R. Brown, C. D. Parker, and E. Yablonovitch, J. Opt. Soc. Am. B **10**, 404 (1993).

[7] D. F. Sievenpiper, M. E. Sickmiller, and E. Yablonovitch, Phys. Rev. Lett. **76**, 2480 (1996).
[8] E. R. Brown and O. B. McMahon, Appl. Phys. Lett. **67**, 2138 (1995).
[9] E. Yablonovitch, T. J. Gmitter, R. D. Meade, A. M. Rappe, K. D. Brommer, and J. D. Joannopoulos, Phys. Rev. Lett. **67**, 3380 (1991).
[10] S. L. McCall, P. M. Platzman, R. Dalichaouch, D. Smith, and S. Schultz, Phys. Rev. Lett. **67**, 2017 (1991).
[11] K. M. Leung, J. Opt. Soc. Am. B **10**, 303 (1993).
[12] N. A. Clark, A. J. Hurd, and B. J. Ackerson, Nature (London) **281**, 57 (1979).
[13] İ. İ. Tarhan and G. H. Watson, Phys. Rev. Lett. **76**, 315 (1996).
[14] İ. İ. Tarhan, M. P. Zinkin, and G. H. Watson, Opt. Lett. **20**, 1571 (1995).
[15] Suspensions of 0.110–0.222-μm diameter (typically 4% standard deviation in the diameter) PS microspheres in water ($\sim$10% PS weight fraction) were obtained from Duke Scientific Corporation, 2463 Faber Place, Palo Alto, CA 94303. The 0.200-μm-diameter ($<$10% standard deviation in diameter) silica particles used as impurity microspheres were obtained from Bangs Laboratories, Inc., 979 Keystone Way, Carmel, IN 46032-2823.
[16] P. Pieranski, Contemp. Phys. **24**, 25 (1983).
[17] The optical stop band width was taken as the difference in frequencies, ν_+ and ν_-, between which the transmission coefficient falls below 10^{-2}. For the undoped crystals, the frequencies ν_+ and ν_- at the 10^{-2} attenuation points agree well with those predicted by an analytical model (Ref. 21).
[18] W. L. Vos *et al.*, Phys. Rev. B **53**, 16 231 (1996).
[19] J. B. Pendry and A. MacKinnon, Phys. Rev. Lett. **69**, 2772 (1992), J. B. Pendry, J. Mod. Opt. **41**, 209 (1994); P. M. Bell *et al.*, Comput. Phys. Commun. **85**, 306 (1995).
[20] *Styrene: Its Polymers, Copolymers and Derivatives*, edited by R. H. Boundy and R. F. Boyer (Hafner Publishing Company, New York, 1965).
[21] İ. İ. Tarhan and G. H. Watson, Phys. Rev. B **54**, 7593 (1996).
[22] K. W.-K. Shung and Y. C. Tsai, Phys. Rev. B **48**, 11 265 (1993).
[23] The refractive index of the silica microspheres according to the manufacturer's (Bangs Labs) quality control data is 1.37, as opposed to densified bulk silica, which is greater than 1.4 for its various crystalline forms.
[24] M. Sigalas, C. M. Soukoulis, E. N. Economou, C. T. Chan, and K. M. Ho, Phys. Rev. B **48**, 14 121 (1993).
[25] J. I. Pankove, *Optical Processes in Semiconductors* (Prentice-Hall, Englewood Cliffs, NJ, 1971).